of migration into a particular region can be eliminated, in part, if similar numbers of immigrants come from the north and the south. However, if more immigrants come from the south, the mean phenotype in a given region will tend to be pushed to a value that is optimal for a more southerly region. It can be shown that the fertility of a local population, in comparison with the fertility of the population immediately to its south, becomes smaller (in proportional terms) as one moves further north. Thus we have another reason why the loss of fitness resulting from migration tends to be largest in the far north.

In the trial shown in Fig. 1a, $\Theta < 1$, so asexuals have an intrinsic fertility disadvantage. Analysis shows that this disadvantage precludes a successful invasion by asexuals with a phenotype that is optimal for region number 5, or by asexuals with phenotypes optimal for any of the regions south of region 5. However, a successful invasion is possible by an asexual phenotype that is optimal for any of the regions north of region 5. This pattern of asexuals being able to invade the initial equilibrium successfully only if they are adapted to northern regions was often found among the polymorphic trials (about 25% of the time). However, we also found that, in about 75% of the polymorphic trials, asexuals optimal for any region could invade the initial equilibrium successfully. Nevertheless, even among these trials, the probability of establishment of a clone after its introduction was generally higher if the clone was adapted to the north and was introduced in the north than if the clone was adapted to the south and introduced in the south.

What accounts for the difference in the likely fate of north- and south-adapted asexual clones? Roughly speaking, members of these clones do not mate, and so individuals with the optimal phenotype for a given region produce offspring with this same optimal phenotype. In contrast, a sexual adult with the locally optimal phenotype may have a non-optimal mate (possibly a migrant), and so many of the offspring may also be non-optimal. Immigrants and their recent descendants are most common in the north, so the initial invasion of asexuals is more likely in northern areas (where their mode of reproduction confers the largest advantage) than in the south. A similar explanation has been proposed to account for the presence of self-fertilizing plants in areas with unusual local environments[21]. Note that a loss of fitness due to maladapted migrants is a well-known phenomenon in natural populations[21,22], and has recently been implicated in speciation and the establishment of the limits of species ranges[23,24].

Throughout the series of invasions that led to the equilibrium shown in Fig. 1a, asexual clones adapted to the far south were at a disadvantage compared with some north-adapted clones (see Fig. 2). The reasons for this are similar to those state above with regard to the initial all-sexual equilibrium.

But what accounts for the 77 polymorphic trials (4%) in which the average position for asexuals was further south than that for sexuals at the final equilibrium? The answer appears to have something to do with the occurrence of unlikely events in the series of invasions leading to the final equilibrium. Strong support for this idea comes from tests in which we re-ran each of the exceptional trials 10 times. In all but 14 of the 77 cases, the average position of sexuals was further south than that of asexuals at the final equilibrium for most of the 10 trials run.

In addition to the simulation study just described, we have also carried out a set of simulations using a model in which the phenotype of the clone that makes the first successful invasion is as described above, but all the subsequent clones are produced as mutations to randomly chosen sexual individuals (just like the first clone), not as mutations to asexual individuals. The results were similar to those described above.

As we have seen, the tendency of the model to produce patterns similar to those found in nature depends on the presence of relatively short growing seasons in the north, and this leads to high frequencies of migrants in northern areas. However, short growing seasons also occur at high altitudes. Thus the processes described here may also explain the tendency of asexuals to occur at high altitudes. Migrants should also be common on the margins of populations because the population density in these areas is often very low compared with nearby (but more central) regions. It has often been asserted that asexuals tend to occur on the margins of populations[2–8], and given our results it seems likely that this is a result of a process similar to the one described above. We have now carried out a simulation study that supports this view (results not shown). □

Received 8 September; accepted 5 November 1997.

1. Vandel, A. La parthéngénèse géographique: contribution l'étude biologique et cytologique de la parthénogénèse naturelle. *Bull. Biol. Belg.* **62,** 164–281 (1928).
2. Suomalainen, E. Parthenogenesis in animals. *Adv. Genet.* **3,** 193–253 (1950).
3. Lynch, M. Destabilizing hybridization, general-purpose genotypes and geographic parthenogenesis. *Q. Rev. Biol.* **59,** 257–290 (1984).
4. Bierzychudek, P. Patterns in plant parthenogenesis. *Experientia* **41,** 1255–1263 (1985).
5. Hughes, R. N. *A Functional Biology of Clonal Animals* (Chapman and Hall, London, 1989).
6. Glesener, R. R. & Tilman, D. Sexuality and the components of environmental uncertainty: Clues from geographic parthenogenesis in terrestrial animals. *Am. Nat.* **112,** 659–673 (1978).
7. Bell, G. *The Masterpiece of Nature* (Univ. California Press, San Francisco, 1982).
8. Parker, E. D. in *Evolutionary Genetics from Molecules to Morphology* (ed. Singh, R. & Krimbas, C.) (Cambridge Univ. Press, in the press).
9. Bulmer, M. *The Mathematical Theory of Quantitative Genetics* (Clarendon, Oxford, 1980).
10. Maynard Smith, J. *The Evolution of Sex* (Cambridge Univ. Press, 1978).
11. Charlesworth, B. Mutation-selection balance and the evolutionary advantage of sex and recombination. *Genet. Res.* **55,** 199–221 (1990).
12. Hamilton, W. D., Axelrod, R. & Tanese, R. Sexual reproduction as an adaptation to resist parasites (a review). *Proc. Natl Acad. Sci. USA* **87,** 3566–3573 (1990).
13. Hurst, L. D. & Peck, J. R. Recent advances in understanding of the evolution and maintenance of sex. *Trends Ecol. Evol.* **11,** 46–52 (1996).
14. Kondrashov, A. S. Deleterioius mutations and the evolution of sexual reproduction. *Nature* **336,** 435–440 (1988).
15. Kondrashov, A. S. Classification of hypotheses on the advantage of amphimixis. *J. Hered.* **84,** 372–387 (1993).
16. Peck, J. R. Frequency dependent selection, beneficial mutations, and the evolution of sex. *Proc. R. Soc. Lond. B* **125,** 87–92 (1993).
17. Peck, J. R. A ruby in the rubbish: Beneficial mutations, deleterious mutations and the evolution of sex. *Genetics* **137,** 597–606 (1994).
18. Peck, J. R. Limited dispersal, deleterious mutations and the evolution of sex. *Genetics* **142,** 1053–1060 (1996).
19. Peck, J. R., Barreau, G. & Heath, S. C. Imperfect genes. Fisherian mutation and the evolution of sex. *Genetics* **145,** 1171–1199 (1997).
20. Michod, R. E. & Levin, B. R. *The Evolution of Sex: an Examination of Current Ideas* (Sinauer, Sunderland, MA, 1988).
21. Antonovics, J. Evolution in closely adjacent plant populations. V. Evolution of self-fertility. *Heredity* **23,** 219–238 (1968).
22. Dias, P. C. Sources and sinks in population biology. *Trends Ecol. Evol.* **11,** 326–330 (1996).
23. Kirkpatrick, M. & Barton, N. H. Evolution of a species range. *Am. Nat.* (in the press). **(Author: update?)**
24. García-Ramos, G. & Kirkpatrick, M. Genetic models of adaptation and gene flow in peripheral populations. *Evolution* **51,** 21–28 (1997).
25. Barton, N. H. The probability of establishment of an advantageous mutant in a subdivided population. *Genet. Res.* **50,** 35–40 (1987).

Acknowledgements. We thank N. H. Barton, B. Charlesworth, J. Maynard Smith, D. Parker and M. Turelli for advice and assistance.

Correspondence and requests for materials should be addressed to J.R.P. at School of Biological Sciences, University of Sussex, Brighton BN1 9QG.

Activity-dependent scaling of quantal amplitude in neocortical neurons

Gina G. Turrigiano, Kenneth R. Leslie, Niraj S. Desai, Lana C. Rutherford & Sacha B. Nelson

Department of Biology and Center for Complex Systems, Brandeis University, Waltham, Massachusetts 02254, USA

Information is stored in neural circuits through long-lasting changes in synaptic strengths[1,2]. Most studies of information storage have focused on mechanisms such as long-term potentiation and depression (LTP and LTD), in which synaptic strengths change in a synapse-specific manner[3,4]. In contrast, little attention has been paid to mechanisms that regulate the total synaptic

strength of a neuron. Here we describe a new form of synaptic plasticity that increases or decreases the strength of all of a neuron's synaptic inputs as a function of activity. Chronic blockade of cortical culture activity increased the amplitude of miniature excitatory postsynaptic currents (mEPSCs) without changing their kinetics. Conversely, blocking GABA (γ-aminobutyric acid)-mediated inhibition initially raised firing rates, but over a 48-hour period mESPC amplitudes decreased and firing rates returned to close to control values. These changes were at least partly due to postsynaptic alterations in the response to glutamate, and apparently affected each synapse in proportion to its initial strength. Such 'synaptic scaling' may help to ensure that firing rates do not become saturated during developmental changes in the number and strength of synaptic inputs[5], as well as stabilizing synaptic strengths during Hebbian modification[6,7] and facilitating competition between synapses[7–9].

We tested the idea that postnatal rat visual cortical pyramidal neurons in primary cell culture scale the strength of AMPA (α-amino-3-hydroxy-5-methyl-4-isoxazole propionic acid)-mediated synaptic currents up or down as a function of activity. To sample inputs from a large number of synapses we used whole-cell voltage-clamp recordings to measure mEPSCs. In control cultures there was a broad distribution of mEPSC amplitudes[10,11] (Fig. 1a; average quantal amplitude = 13.6 ± 0.7 pA at −70 mV, $n = 27$). The effects of decreasing or increasing firing rates for 48 h on mEPSC amplitude are shown in Fig. 1a. On average, mEPSC amplitudes from cultures grown in tetrodotoxin (TTX), which completely abolished firing, increased to 192 ± 16% of control values, and there was a similar effect on area (Fig. 1b, $n = 10$). Blockade of $GABA_A$-mediated inhibition with bicuculline, which raised firing rates to 265 ± 10% of control values, significantly decreased mEPSC amplitude to 70 ± 4% of control values (Fig. 1b, $n = 10$), and also decreased mEPSC area. For the manipulations described here and below, resting potentials, input resistances, whole-cell capacitances and series resistances were similar between conditions (Table 1). These data demonstrate that the quantal amplitude of AMPA synapses can be increased or decreased by changes in activity. Activity blockade did not significantly affect the amplitude of AMPA-mediated mEPSCs recorded from bipolar interneurons (Fig. 1c, $n = 14$), indicating that excitatory inputs from pyramidal neurons are regulated differently depending on the nature of the target neuron.

Some forms of synaptic plasticity require calcium influx through NMDA (*N*-methyl-D-aspartate) receptors[3,4]. To examine the effects of NMDA receptor blockade on mEPSC amplitude, cultures were grown in the NMDA antagonist AP5 (D(−)-amino-7-phosphonovalenic acid) for 48 h AP5 did not influence firing rates (95 ± 24% of control values), and had no effect on mEPSC amplitude or area (Fig. 1b, $n = 8$). In contrast, blocking AMPA receptors with 6-cyano-7-nitroquinoxaline-2,3-dione (CNQX), which like TTX completely abolished firing, significantly increased mEPSC amplitude to 195 ± 24% of control values (Fig. 1b, $n = 10$). These observations indicate that, in contrast to many forms of LTP and LTD[3,4,12], the change in synaptic strength produced by activity blockade is not simply the result of a change in NMDA receptor signalling.

Cumulative amplitude histograms showed that the entire distribution of mEPSC amplitudes shifted towards larger values for

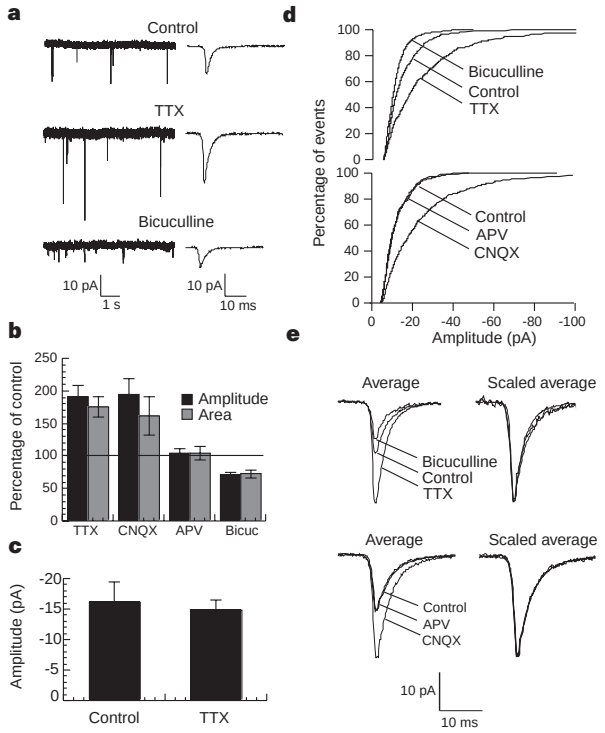

Figure 1 AMPA mEPSC amplitudes from control cultures or cultures grown in TTX, CNQX or bicuculline for 48 hours. **a**, Representative recordings. Left, raw data; right, average mEPSC waveform for the neuron on the left. **b**, Average mEPSC amplitudes and areas expressed as a percentage of control (one way analysis of variance (ANOVA), $P < 0.002$); *t*-tests (using a Bonferoni correction for multiple comparisons) indicate that TTX, CNQX and bicuculline (Bicuc) amplitudes differ significantly from control ($P < 0.004$, 0.02 and 0.01, respectively), whereas AP5 does not. **c**, Average amplitudes of AMPA mEPSCs from bipolar interneurons grown with or without TTX for 48 h. **d**, Cumulative amplitude histograms for mEPSCs recorded under each condition. **e**, Average mEPSC waveforms for each condition, unscaled (average) and scaled (scaled average).

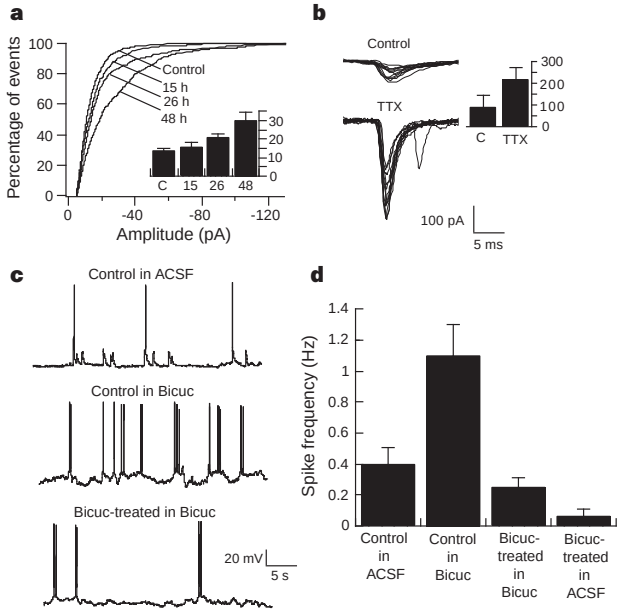

Figure 2 Effects of activity on mEPSCs, paired transmission, and firing rates. **a**, Time course of changes in quantal amplitude. Inset, mean mEPSC amplitudes for control and after 15, 26 and 48 h (one way ANOVA, $P < 0.002$). **b**, Paired recordings from control and TTX-treated cultures. Inset, mean ± s.e.m. for control ($n = 13$) or TTX-treated ($n = 9$, $P < 0.005$, Wilcoxon rank sum test) pairs. **c**, **d**, Regulation of firing rates during chronic exposure to bicuculline. Control cultures recorded in ACSF or bicuculline (Bicuc), and bicuculline-treated cultures recorded in bicuculline or ACSF. **c**, Representative recordings. **d**, mean ± s.e.m. ($n = 9$ in each condition; Bicuc in Bicuc significantly different from control in Bicuc, $P < 0.01$, and not significantly different from control in ACSF, $P = 0.24$, corrected *t*-test).

TTX-treated and CNQX-treated cultures, and towards smaller values for bicuculline-treated cultures (Fig. 1d). We examined mEPSC kinetics by determining the average mEPSC waveforms under the different conditions (Fig. 1e). Scaling and overlaying these averaged waveforms revealed no differences in the rise and decay kinetics (Fig. 1e), and individual measurements of rise times also showed no significant differences between conditions (Table 1). In contrast to LTP and other rapid potentiation protocols[13–15], there were no significant differences in mEPSC frequency between conditions (Table 1). The lack of effect on frequency and kinetics suggests that, in accord with other studies[16,17], altering activity for two days does not significantly influence the placement or number of excitatory synapses onto pyramidal neurons.

The time course of mEPSC regulation was determined by blocking activity for 15, 26, or 48 (±4) h ($n = 8$, 11 and 10, respectively). There was a progressive increase in mEPSC amplitude with treatment time, indicating that this process is both slow and cumulative (Fig. 2a).

Does the activity-dependent regulation of mEPSC amplitude produce a change in spike-mediated EPSCs? TTX treatment increased EPSC amplitude between pairs of monosynaptically connected pyramidal neurons from 89 ± 65 pA (measured at −70 mV, $n = 13$ pairs) to 219 ± 52 pA ($n = 9$ pairs) (Fig. 2b). There was no effect on EPSC reversal potential (1.6 ± 1.0 and 2.2 ± 1.1 mV for control and TTX-treated pyramidal neurons, respectively).

The regulation of mEPSC amplitudes described above could act to stabilize firing rates, because raising firing rates decreases the strength of excitatory synaptic inputs, and vice versa. To test whether firing rates are regulated homeostatically in response to changes in activity, cultures were grown under control conditions or in bicuculline for 48 h, and whole-cell current-clamp recordings were used to measure firing rates (Fig. 2c). Acute bicuculline treatment raised firing rates significantly from 0.4 ± 0.1 to 1.1 ± 0.2 Hz (Fig. 2d), but after 48 h in bicuculline, firing rates recorded in bicuculline declined significantly to 0.24 ± 0.06 Hz, and were close to zero when bicuculline was removed (Fig. 2d). These data indicate that increased firing produces a regulatory response that returns firing rates to control levels. Previous studies have shown that chronic TTX treatment dramatically increases firing rates when the TTX is removed[18,19]. The bidirectional regulation of

Table 1 Effects of treatments on neuronal properties

Treatment	V_m	R_{in}	Rise time	Capacitance	S_r	Frequency
TTX	99.8 ± 3.5	113.0 ± 19.0	91.6 ± 8.4	104.1 ± 11.7	101.1 ± 9.7	95.5 ± 15.5
CNQX	105.5 ± 4.2	108.4 ± 18.2	92.8 ± 6.4	95.5 ± 9.2	83.6 ± 8.9	99.2 ± 26.0
Bicuculline	103.5 ± 2.3	100.3 ± 14.0	103.5 ± 2.3	99.8 ± 8.6	110.4 ± 6.6	108.2 ± 22.3
AP5	102.3 ± 2.6	102.3 ± 5.0	91.6 ± 9.7	104.7 ± 11.7	100.2 ± 11.2	99.5 ± 26.5

Effects of treatment on resting potential (V_m), input resistance (R_{in}), mEPSC rise times, whole-cell capacitance, series resistance (S_r) and mEPSC frequency, expressed as a percentage of values from sister control cultures. None of these differences were statistically significant. For controls, $V_m = 60.3 \pm 1.6$ mV; $R_m = 1.1 \pm 0.4$ GΩ; rise time = 0.78 ± 0.05 ms; capacitance = 28.7 ± 3.9 pF; $S_r = 12.8 \pm 1.2$ MΩ; and mEPSC frequency = 0.34 ± 0.08 Hz.

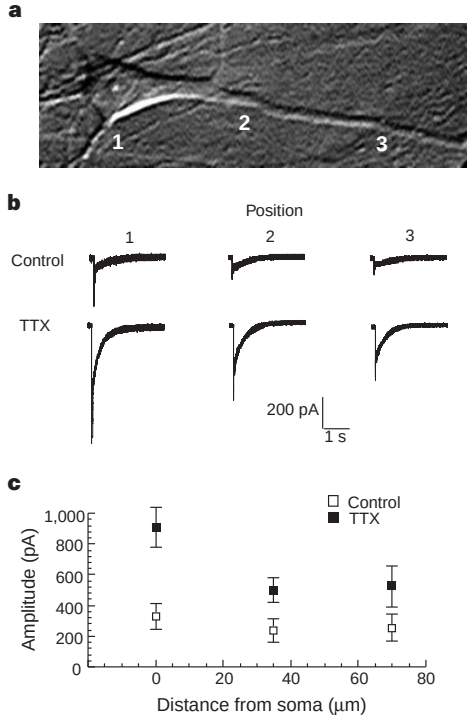

Figure 3 Activity blockade increases the postsynaptic sensitivity to glutamate. **a**, Differential interference contrast image of a cultured pyramidal neuron, showing the sites at which glutamate was applied: 1, soma; 2, 35 μm from the soma; and 3, 70 μm from the soma. **b**, Representative responses for control and TTX-treated neurons: 1, 2 and 3 correspond to the sites indicated in **a**. Each trace shows 5 overlaid responses from the same site. **c**, Average responses at the three sites for control ($n = 9$) and TTX-treated ($n = 8$) neurons. Responses for TTX-treated neurons are significantly larger than control (site 1, $P < 0.001$; 2, $P < 0.02$; 3, $P < 0.05$, t-test).

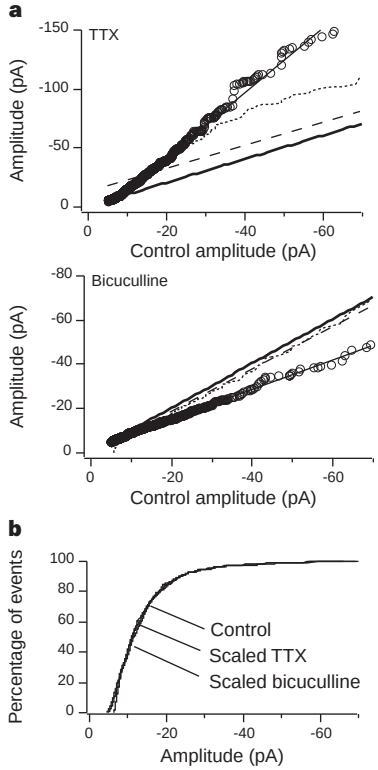

Figure 4 Activity scales mEPSC amplitudes multiplicatively. **a**, Ranked control amplitudes were plotted against ranked TTX or bicuculline amplitudes, and the best fit to the data (open circles) of additive (dashed lines), random additive (dotted curves), or multiplicative (thin solid lines) functions was determined. Thick solid lines are control plotted against control, and have slopes of 1. Best fit: TTX = control × 2.73 + 12.3, $R = 0.997$; Bicuculline = control × 0.66 − 2.0, $R = 0.998$. **b**, The original TTX and bicuculline distributions were transformed by the preceding equations and plotted with the control data.

quantal amplitude is likely to contribute significantly to the homeostatic regulation of firing rates.

Changes in mEPSC amplitude could be occurring through a postsynaptic change in glutamate responsiveness or a presynaptic change in the glutamate content of synaptic vesicles. To investigate this, pulses of glutamate were applied to pyramidal neurons in the presence of TTX and AP5 and the amplitudes of the resulting glutamate currents were measured (Fig. 3a, b). Chronic TTX treatment increased the current amplitude to 278 ± 39% of control values at the soma, and similar increases were seen along the apical dendrite (Fig. 3c; control, $n = 9$; TTX, $n = 8$). No difference in rise times or times to peak of the glutamate currents were observed between conditions, indicating that the difference in amplitude is not due to a difference in rates of diffusion or removal of glutamate under the two conditions (rise times = 7.5 ± 0.7 and 8.9 ± 0.8 ms, and times to peak = 23 ± 1.4 and 25 ± 1.1 ms, respectively). These data suggest that activity regulates mEPSC amplitude through a postsynaptic change in receptor number or function, although there may be additional presynaptic changes. In contrast to supersensitivity at the neuromuscular junction, where enhanced responsiveness is exclusively extrajunctional and mEPP amplitude does not change[20,21], the change in mEPSC amplitude observed here indicates that receptors located at the synapse are involved in the regulatory process.

What is the relationship between the mEPSC amplitude distributions produced by different activity levels? The average quantal amplitude could be modified by changing synaptic strengths by a constant value (an additive function), by adding a random amount (a random additive function), or by scaling synaptic strengths by the same multiplicative factor (a multiplicative function). To distinguish between these possibilities, control amplitudes were plotted against TTX amplitudes (Fig. 4a) or bicuculline amplitudes (Fig. 4b) and the resulting relationship fit using each of the above models. The data were well fit by linear functions with slopes of 2.73 (TTX) and 0.66 (bicuculline), but not by additive or random additive functions (Fig. 4a). When scaled multiplicatively by these slope values, the cumulative amplitude distributions for TTX and bicuculline were almost perfectly superimposable on the control distribution (Fig. 4b), suggesting that activity is globally scaling quantal amplitudes in a multiplicative manner. Taken together, our data place several constraints on the biophysical mechanism of synaptic scaling. If this scaling occurs through a change in the function of existing AMPA receptors through phosphorylation[22,23] or some other mechanism, this process must modify single-channel conductance without influencing mEPSC kinetics. Alternatively, if this scaling occurs through changes in the synthesis and insertion of glutamate receptors[24,25], or through conversion of existing receptors between inactive and active states[26,27], then receptors must be inserted or converted in proportion to the existing number of functional receptors.

Multiplicative scaling of synaptic strengths preserves relative differences between inputs (such as those produced by Hebbian modifications), while allowing a neuron to adjust the total amount of synaptic excitation it receives. This process may help developing neurons remain responsive to inputs both early in development, when the number of synaptic inputs is small, and later in development as the number rises[28]. This may be important for allowing developing neurons to participate in the correlation-based mechanisms that contribute to circuit formation[5]. Consistent with this, there is evidence that mEPSC amplitudes in hippocampal neurons decrease as the number of synaptic inputs increase[29]. In addition, by contributing to a stabilization in firing rates, synaptic scaling may help to counteract the destabilizing effects of Hebbian synaptic modifications[6,7,30]. This instability arises because synaptic potentiation increases postsynaptic firing rates, thus increasing the correlation with presynaptic activity and producing a positive feedback loop that eventually saturates even weakly correlated inputs. Finally, this process predicts that strengthening of some inputs will lead to a scaling down of all synaptic strengths. Synaptic weakening has been suggested to be the prelude to synapse elimination[8,9]. By reducing weak inputs in response to the strengthening of others, synaptic scaling may contribute to the processes of synaptic competition and elimination. □

Methods

Rat visual cortical cultures were prepared from rat pups at postnatal days 4–6, and whole-cell recordings were obtained in artificial cerebrospinal fluid (ACSF) as described[18]. Experiments were performed after 7–9 days *in vitro*. All data were obtained in parallel on treated and age-matched sister control cultures. Drug concentrations were 1 μM TTX, 20 μM bicuculline, 20 μM CNQX and 50 μM AP5. Recordings with resting potentials greater than −55 mV, series resistances greater than 20 MΩ, or fewer than 50 mEPSCs were excluded. Pyramidal and non-pyramidal neurons were distinguished as described[18]. To record mEPSCs, neurons were held in voltage clamp at −70 mV using an Axopatch 1D in the presence of TTX, bicuculline and AP5. In-house software was used to detect and measure mEPSCs; detection criteria included amplitudes greater than 5 pA and 20–80% rise times less than 3 ms. All data are reported as mean ± s.e.m. for the number of neurons indicated. Paired recordings were obtained in ACSF with AP5, and the pipette solution for the postsynaptic cell contained caesium and QX-314. Monosynaptic EPSCs were considered to be those with latencies of less than 4 ms, less than 1 ms of jitter, a monotonic rising phase, and reversal potentials of approximately 0 mV. A picospritzer was used to deliver puffs of 0.5 mM glutamate (pipette diameter, 2 μm) while holding pyramidal neurons at −70 mV in whole-cell voltage clamp in the presence of TTX and AP5. Puffs were repeated 5 times at each site and the results averaged. The relationship between control and experimental amplitude distributions was determined by ranking mEPSC amplitudes from all cells recorded from TTX-treated, bicuculline-treated, or control cultures in ascending order. These amplitude distributions were linearly interpolated to produce an equal number of observations in each condition, and experimental amplitudes plotted against control amplitudes. For additive function, the same value was added to each control amplitude; for random additive functions, the differences between ranked experimental and control amplitudes were calculated and these values were added to control amplitudes in random order; for multiplicative functions, each control value was transformed by a linear equation with a slope greater than (for TTX) or less than (bicuculline) 1; the non-zero intercepts of the best-fit multiplicative functions are close to those required (8.7 and −1.7 pA, respectively) to compensate for the 5-pA amplitude cut-offs.

Received 5 November 1997; accepted 19 January 1998.

1. Hebb, D. O. *The Organization of Behavior: a Neurophysiological Theory* (Wiley, New York, 1949).
2. Stent, G. S. A physiological mechanism for Hebb's postulate of learning. *Proc. Natl Acad. Sci. USA* **70,** 997–1001 (1973).
3. Madison, D. V. *et al.* Mechanisms underlying long-term potentiation of synaptic transmission. *Annu. Rev. Neurosci.* **14,** 379–397 (1991).
4. Linden, D. J. & Connor, J. A. Long-term synaptic depression. *Annu. Rev. Neurosci.* **18,** 319–357 (1995).
5. Shatz, C. J. Impulse activity and the patterning of connections during CNS development. *Neuron* **5,** 745–756 (1990).
6. Bienenstock, E. L. *et al.* Theory for the development of neuron selectivity: orientation specificity and binocular interaction in visual cortex. *J. Neurosci.* **2,** 32–48 (1982).
7. Miller, K. D. Synaptic economics: competition and cooperation in synaptic plasticity. *Neuron* **17,** 371–374 (1996).
8. Lo, Y. J. & Poo, M. Activity-dependent synaptic competition in vitro: heterosynaptic suppression of developing synapses. *Science* **254,** 1019–1022 (1991).
9. Colman, H. *et al.* Alterations in synaptic strength preceding axon withdrawal. *Science* **275,** 356–361 (1997).
10. Bekkers, J. M. *et al.* Origin of variability in quantal size in cultured hippocampal neurons and hippocampal slices. *Proc. Natl Acad. Sci. USA* **87,** 5359–5362 (1990).
11. Hestrin, S. Activation and desensitization of glutamate-activated channels mediating fast excitatory synaptic currents in the visual cortex. *Neuron* **9,** 991–999 (1992).
12. Kirkwood, A. & Bear, M. F. Hebbian synapses in visual cortex. *J. Neurosci.* **14,** 1634–1645 (1994).
13. Manabe, T. *et al.* Postsynaptic contribution to long-term potentiation revealed by the analysis of miniature synaptic currents. *Nature* **355,** 50–55 (1992).
14. Malgaroli, A. *et al.* Glutamate-induced long-term potentiation of the frequency of miniature synaptic currents in cultured hippocampal neurons. *Nature* **357,** 134–139 (1992).
15. Wyllie, D. J. *et al.* A rise in postsynaptic calcium potentiates miniature excitatory postsynaptic currents and AMPA responses in hippocampal neurons. *Neuron* **12,** 127–138 (1994).
16. Micheva, K. D. & Beaulieu, C. An anatomical substrate for experience-dependent plasticity of the rat barel field cortex. *Proc. Natl Acad. Sci. USA* **92,** 11834–11838 (1995).
17. Benson, D. L. & Cohen, P. A. Activity-independent segregation of excitatory and inhibitory synaptic terminals in cultured hippocampal neurons. *J. Neurosci.* **16,** 6424–6432 (1996).
18. Rutherford, L. C. *et al.* BDNF mediates the activity-dependent regulation of inhibition in neocortical cultures. *J. Neurosci.* **17,** 4527–4535 (1997).

19. Ramakers, G. J. A. *et al.* Development in the absence of spontaneous bioelectric activity results in increased stereotyped burst firing in cultures of dissociated cerebral cortex. *Exp. Brain Res.* **79,** 157–166 (1990).
20. Axelsson, J. & Thesleff, S. A study of supersensitivity in denervated mammalian skeletal muscle. *J. Physiol. (Lond.)* **149,** 178–193 (1957).
21. Berg, D. K. & Hall, Z. W. Increased extrajunctional acetylcholine sensitivity produced by chronic post-synaptic neuromuscular blockade. *J. Physiol (Lond.)* **244,** 659–676 (1975).
22. McGlade-McCulloh, E. *et al.* Phosphorylation and regulation of glutamate receptors by calcium/calmodulin-dependent protein kinase II. *Nature* **362,** 640–642 (1993).
23. Barria, A. *et al.* Regulatory phosphorylation of AMPA-type glutamate receptors by CaM-KII during long-term potentiation. *Science* **276,** 2042–2045 (1997).
24. Gerfin-Moser, A. *et al.* Alterations in glutamate but not GABAA receptor subunit expression as a consequence of epileptiform activity in vitro. *Neuroscience* **67,** 849–865 (1995).
25. Liang, F. & Jones, E. G. Differential and time-dependent changes in gene expression for type II calcium/calmodulin-dependent protein kinase, 67 kDa glutamic acid decarboxylase, and glutamate receptor subunits in tetanus toxin-induced focal epilepsy. *J. Neurosci.* **17,** 2168–2180 (1997).
26. Liao, D. *et al.* Activation of postysnaptically silent synapses during pairing-induced LTP in CA1 region of hippocampal slice. *Nature* **375,** 400–404 (1995).
27. Wu, G.-Y. *et al.* Maturation of a central glutamatergic synapse. *Science* **274,** 972–976 (1996).
28. Blue, M. E. & Parnavelas, J. G. The formation and maturation of synapses inthe visual cortex of the rat. II. Quantitative analysis. *J. Neurocytol.* **12,** 697–712 (1983).
29. Liu, G. & Tsien, R. W. Properties of synaptic transmission at single hippocampal synaptic boutons. *Nature* **375,** 404–408 (1995).
30. Miller, K. D. & MacKay, D. J. C. The role of constraints in Hebbian learning. *Neur. Comput.* **6,** 100–126 (1993).

Acknowledgements. We thank H. Lauer for technical assistance, and L. F. Abbott, J. Lisman, E. Marder and M. Mauk for discussions and advice. This work was supported by the Whitehall Foundation, NSF, NIH and the Sloan Foundation. K.R.L. was supported by an HHMI predoctoral fellowship.

Correspondence and requests for materials should be addressed to G.G.T. (e-mail: turrigiano@binah.cc.brandeis.edu).

Molecular characterization of a neuronal low-voltage-activated T-type calcium channel

Edward Perez-Reyes*†, Leanne L. Cribbs*†, Asif Daud*, Antonio E. Lacerda‡, Jane Barclay§, Magali P. Williamson§, Margaret Fox‖, Michele Rees§ & Jung-Ha Lee*

** Department of Physiology, and †Cardiovascular Institute, Loyola University Medical Center, Maywood, Illinois 60153, USA*
‡ Rammelkamp Center for Research & Education, MetroHealth Medical Center, Cleveland, Ohio 44109, USA
§ Department of Paediatrics, The Rayne Institute, University College London Medical School, London WC1E 6JJ, UK
‖ MRC Human Biochemical Genetics Unit, The Galton Laboratory, London NW1 2HE, UK

The molecular diversity of voltage-activated calcium channels was established by studies showing that channels could be distinguished by their voltage-dependence, deactivation and single-channel conductance[1–3]. Low-voltage-activated channels are called 'T' type because their currents are both transient (owing to fast inactivation) and tiny (owing to small conductance)[2]. T-type channels are thought to be involved in pacemaker activity, low-threshold calcium spikes, neuronal oscillations and resonance, and rebound burst firing[4]. Here we report the identification of a neuronal T-type channel. Our cloning strategy began with an analysis of Genbank sequences defined as sharing homology with calcium channels. We sequenced an expressed sequence tag (EST), then used it to clone a full-length complementary DNA from rat brain. Northern blot analysis indicated that this gene is expressed predominantly in brain, in particular the amygdala, cerebellum and thalamus. We mapped the human gene to chromosome 17q22, and the mouse gene to chromosome 11. Functional expression of the channel was measured in *Xenopus* oocytes. Based on the channel's distinctive voltage dependence, slow deactivation kinetics, and 7.5-pS single-channel conductance, we conclude that this channel is a low-voltage-activated T-type calcium channel.

The molecular biology of voltage-activated Ca^{2+} channels began with the cloning of the skeletal muscle dihydropyridine receptor, α1S (reviewed in ref. 5). Using a combination of low-stringency hybridization and polymerase chain reaction (PCR) techniques, five other α1 subunits of calcium channels have been cloned[5]. All six of these α1 subunits form high-voltage-activated (HVA) Ca^{2+} channels. Original studies on a rat α1E clone[6] suggested that it belonged to the low-voltage-activated (LVA) family. However, mouse[7], rabbit[8] and human[7,9] α1E clones form HVA channels. Strong evidence that α1E is not part of a T-type channel was provided by studies showing it had double the single channel conductance for Ba^{2+} (12–14 pS)[7–10]. Our alternative cloning strategy was to use a text-based search of the Genbank to find new sequences that showed homology with cloned calcium channels. Based on its 45% homology with domain III S1 of the carp α1 (P22316), we decided to sequence H06096. Although its deduced amino-acid sequence had low homology to cloned Ca^{2+} channels, it contained readily identifiable motifs including an S4 region and a pore loop. Using H06096 as a probe, we screened a rat brain λgt10 cDNA library. A full-length cDNA, referred to as α1G or Ca_vT.1, was assembled from five overlapping clones. Search of the non-redundant division of the Genbank revealed that α1G was similar to other Ca^{2+} channel α1 subunits, but most similar to C54D2.5 (Genbank No. U37548), a putative protein found in the genomic DNA of *Caenorhabditis elegans*[11]. Homologous human (H19230, R19524) and mouse (AA386626) EST clones were also identified and sequenced. Sequence identity among the Ca^{2+} channel α1 subunits is highest in the putative membrane-spanning regions, with most changes being conservative with respect to structure (Fig. 1). Charged residues are particularly conserved, with many charges being conserved across all domains and in voltage-gated Na^+ and K^+ channels[12]. The charged residues of the S4 regions are also conserved, consistent with its role as a voltage sensor[13]. The cation selectivity of Ca^{2+} channels requires a ring of negative charge provided by glutamate residues found at similar locations in each domain[14]. In α1G, two of these glutamates are replaced by aspartate, suggesting an altered selectivity. In contrast, there is little conservation of the sequences that link these regions within a domain, and even less between the intracellular loops that connect the domains. Notably, the motifs involved in binding the β-subunit[15,16] and calcium[17] are missing.

Northern blot analysis of human and rat tissues indicates there are two α1G messenger RNA transcripts, with a predominant band of 8.5 kilobases (kb) and another of 9.7 kb (Fig. 2). The strongest signals were detected in brain, and less abundantly in heart. Longer exposure reveals expression in placenta, kidney and lung. Transcripts were detected in all human brain regions studied, with strong signals from (in relative order of abundance) amygdala, thalamus, subthalamic nuclei (Fig. 2c) and cerebellum (data not shown). To confirm the northern blot analysis, we used PCR followed by subcloning and sequencing.

Genetic mutations of either the calcium channel α1A subunit or β_4 subunits result in ataxic and epileptic phenotypes[18,19]. A similar link between T-type channels and absence epilepsy has been suggested[20]. As a first step in exploring such a link we mapped the human and murine α1G genes. The human α1G gene, *CACNA1G*, was mapped to chromosome 17 between the markers AFMA126YD5 and D17S798 (LOD score > 3.0), using the Genbridge 4 radiation hybrid panel. Fluorescent *in situ* hybridization to normal male human metaphase spreads was carried out using the α1G cDNA clone R19524. Analysis of 22 metaphases confirmed the localization of *CACNA1G* to chromosome 17 and 59% of these could be assigned to the 17q22 band. The mouse α1G gene, *Cacna1g*, was mapped to chromosome 11 on the EUCIB map[21] between the markers JPAV507 and D11Mit263 with a LOD score of 8.0.